https://doi.org/10.5194/egusphere-2024-2065
Preprint. Discussion started: 23 August 2024
© Author(s) 2024. CC BY 4.0 License.

Dust storms transport proteinaceous matter from the Gobi Desert to Northern China

Ren-Guo Zhu[1,2], Hua-Yun Xiao[3,*], Meiju Yin[3], Hao Xiao[3], Zhongkui Zhou[1], Yuanyuan Pan[1], Guo Wei[1], Cheng Liu[1]

[1]School of Water Resources and Environmental Engineering, East China University of Technology, Nanchang 330013, China.
[2]Jiangxi Provincial Key Laboratory of Genesis and Remediation of Groundwater Pollution, East China University of Technology, Nanchang 330013, China.
[3]School of Agriculture and Biology, Shanghai Jiao Tong University, Shanghai 200240, China.

Corresponding author: Hua-Yun Xiao (Xiaohuayun@sjtu.edu.cn)

Abstract. Dust storms can greatly influence the ecosystem's productivity and biogeochemical nitrogen cycles by providing new nutrients. However, the transport of proteinaceous matter (combined amino acids, CAAs) by dust storms to downwind ecosystems remains unclear. Here, the concentrations and $\delta^{15}N$ values of individual CAAs in Gobi surface soil and vegetation, as well as in $PM_{2.5}$ samples from four cities in Northern China were characterized. Proline dominated the total pool of CAAs in urban $PM_{2.5}$ during non-dust periods, whereas CAAs transported by Gobi dust were rich in alanine, glycine, and glutamic acid. The concentrations and percentages of these three CAAs in $PM_{2.5}$ from Northern China notably increased during dust periods. During non-dust periods, the $\delta^{15}N$ values of individual CAAs in urban $PM_{2.5}$ fell within their respective ranges in local urban sources, suggesting CAAs in $PM_{2.5}$ were primarily influenced by local urban sources during non-dust periods. Compared to their values in urban $PM_{2.5}$ during non-dust periods, glycine and leucine in Gobi Desert sources exhibited $\delta^{15}N$ depletion by more than 6‰. During dust periods, glycine and leucine in urban $PM_{2.5}$ all exhibited negative shifts in their $\delta^{15}N$ values, confirming that Gobi dust is a significant source of CAAs in $PM_{2.5}$ in Northern China. The dry deposition of protein-N from Gobi dust was calculated using nitrogen isotopic mass balance based on the $\delta^{15}N$ values of glycine and leucine, yielding a value of up to 0.36 mg N m^{-2} d^{-1}. The rapid accumulation of such considerable protein-N quantities may profoundly affect oligotrophic ecosystem productivity.

https://doi.org/10.5194/egusphere-2024-2065
Preprint. Discussion started: 23 August 2024
© Author(s) 2024. CC BY 4.0 License.

1 Introduction

Asian dust storms, originating from the desert and Gobi regions of Inner Mongolia in China and southern Mongolia, are a significant source of atmospheric particulate matter, annually emitting approximately 1000-3000 teragrams (Tegen and Schepanski, 2009). Recent studies indicate that, in addition to mineral dust, these storms can transport substantial amounts of water-soluble organic nitrogen (WSON) to urban aerosols and even distant oceans (Liu et al., 2021; Mochizuki et al., 2016; Tsagkaraki et al., 2021). Importantly, primary biological particles present in desert soils can be lifted by dust storm into the stratosphere and transported over long distances (Favet et al., 2013).

Combined amino acids (CAAs), including proteins and peptides, are important constituents of atmospheric organic nitrogen (Jaenicke, 2005; Zhang and Anastasio, 2003). Recent studies reveal that they are ubiquitous in aerosols across various environments such as urban, suburban, rural, and remote areas (Li et al., 2022a; Li et al., 2022b). Protein-containing particles are expected to influence particle hygroscopicity, atmospheric chemistry, cloud formation processes and new particle formation and growth (Chan et al., 2005; Elbert et al., 2007; Haan et al., 2009; Jaber et al., 2021; Violaki and Mihalopoulos, 2010). Moreover, they serve as bioavailable nitrogen sources and greatly contribute to the biogeochemical nitrogen cycles (Matsumoto et al., 2017; Neff et al., 2002). Therefore, the nutrient enrichment resulting from dry deposition of proteinaceous matter attract attention in aerosol studies (Samy et al., 2013; Xu et al., 2020; Zhang and Anastasio, 2003).

However, the sources of CAAs in aerosols remain insufficiently elucidated. Generally, the suspension process of biological particles, including fungi, spores, bacteria, molds, animal dander, pollen, and fragments of plants and animals, along with soil particles, has been identified as primary sources of CAA in aerosols (Filippo et al., 2014; Matos et al., 2016; Samy et al., 2013). Besides that, atmospheric proteins are also suggested to originate from biomass burning (Kang et al., 2012; Song et al., 2017; Zhu et al., 2020a) and marine sources, such as bursting sea bubbles and suspended algae (Feltracco et al., 2019; Li et al., 2022a; Triesch et al., 2021). However, Matsumoto et al. (2021) found a significant correlation between the total CAAs concentration in fine particles at an urban site in Japan and the concentration of non-sea-salt calcium (nss-Ca^{2+}), suggesting an influence of Asian dust particles on airborne CAAs. To date, no studies have directly compared the protein characteristics in $PM_{2.5}$ from urban environments

https://doi.org/10.5194/egusphere-2024-2065
Preprint. Discussion started: 23 August 2024
© Author(s) 2024. CC BY 4.0 License.

with those in dust sources to conclusively determine the contribution of dust sources to proteinaceous materials in downwind urban $PM_{2.5}$ during dust events.

Composition profiles of CAAs have been utilized to identify emission sources of primary biological aerosol particles (Abe et al., 2016; Matsumoto et al., 2021). Zhang and Anastasio (2003) noted a significant contribution of serine to the total CAAs pool in the $PM_{2.5}$, highlighting the direct emissions from biological sources such as plants and animals. Matsumoto et al. (2021) identified glutamic acid, glycine, and aspartic acid as the dominant amino acids in the total CAAs pool in fine aerosols, indicating that regional and locally derived biomass burning and fossil fuel combustion are the sources of CAAs in fine atmospheric particles. Moreover, our previous study suggested distinct differences between the CAA composition profiles in surface soil and plant sources; hydrophobic species (alanine, valine, leucine, and isoleucine) and neutral proline were the major CAA species in soil sources, while hydrophilic CAA species (glutamic acid, lysine, and aspartic acid) represented major fractions in plant sources (Zhu et al., 2020b). Unfortunately, the composition profiles of CAAs in distant dust sources and local urban aerosols remain inadequately characterized.

With the development of stable N isotope technology, compound-specific isotope analysis of amino acids has become an effective tool to trace the sources and cycling of dissolved organic nitrogen in marine environment (Batista et al., 2014; Ianiri and Mccarthy, 2023; Yamaguchi and Mccarthy, 2018). In atmospheric studies, $\delta^{15}N$ values of glycine have been employed as a novel method to identify the sources of proteinaceous matter in aerosols (Zhu et al., 2021). Our previous study suggested that the $\delta^{15}N$ values of Gly in aerosol particles from biomass burning sources (averaged +22.4±4.4‰) were more positive than those of soil (averaged +5.2±3.5‰) and plant sources (averaged -13.4‰) (Zhu et al., 2020b). Therefore, according to the $\delta^{15}N$ inventories of specific CAAs in potential emission sources, the main sources of CAAs in atmospheric particles could be identified. Changes in $\delta^{15}N$ values of specific CAAs in the aerosols could be close related to the variation in the primary emission sources of atmospheric proteinaceous matter (Zhu et al., 2020b). However, limited knowledge on the $\delta^{15}N$ inventories of individual CAAs in dust sources and local urban sources complicates the elucidation of CAA origins in urban $PM_{2.5}$ on dusty days.

The overall goal of this present study was to evaluate the contribution of the Gobi dust sources to the proteinaceous matter (CAAs) in $PM_{2.5}$ from four representative urban in Northern China on dusty days.

https://doi.org/10.5194/egusphere-2024-2065
Preprint. Discussion started: 23 August 2024
© Author(s) 2024. CC BY 4.0 License.

Firstly, we analyzed the concentrations and $\delta^{15}N$ values of individual CAAs in the surface soil and prevalent plants in the Gobi Desert, along with surface soil and the predominant plant species in Beijing, Tianjin, Shijiazhuang, and Taiyuan. The objective was to examine the composition characteristics and nitrogen isotope signature of individual CAAs from both Gobi dust sources and local urban sources; Secondly, variations in the concentrations and $\delta^{15}N$ values of CAAs in $PM_{2.5}$ samples from these four cities during non-dust and dust periods were analyzed to confirm whether Gobi dust sources contribute to CAAs in $PM_{2.5}$ in Northern China and to quantify the extent of this contribution for each city. Finally, we quantified the dry deposition of protein-N transported by the dust storm. This work could potentially improve current knowledge on the influence of Asian dust storms on productivity and biogeochemical nitrogen cycles in downwind ecosystems.

2 Materials and Methods

2.1 Sample collection

An intensive ground monitoring network consisting of four sites (Beijing, Tianjin, Shijiazhuang, and Taiyuan) in Northern China was set up to monitor the dust episodes (Figure S1). The MODIS satellite image (https://worldview.earthdata.nasa.gov/), as shown in Figure S1, shows a dust episode with brown dust plumes clearly visible over these four sampling sites.

The $PM_{2.5}$ samples on quartz fiber filters were simultaneously collected at Beijing, Tianjin, Shijiazhuang, and Taiyuan by a high-volume air sampler (KC-1000, Qingdao Laoshan Electronic Instrument company, China) at a flow rate of 1.05 ± 0.03 m^3 min^{-1}. The high-volume air sampler was set on the rooftop of a building (approximately 12 m above ground) at each site. Quartz filters were pre-combusted at 450 °C for 10 hours; then wrapped in pre-combusted (450 °C, 10hr) aluminum foil envelopes and placed in separate plastic bags. Daily $PM_{2.5}$ samples were collected from March 24, 2018 to 1 from March 31, 2018 at four cities. The sampling duration time for each sample was generally 23.5 h from 9:00 to 8:30 LT (local time) of the next day. All sample filters were sealed individually in an aluminum foil bag and stored at -20°C prior to analysis. Field blank samples were also collected and analyzed as the control.

Surface soil samples (0-10 cm) and leaves from three common plants, *chenopodium ambrosioides, Tripogon chinensis, and tamarix chinensis*, were collected in the Gobi area (115.1°E, 28.2°N), situated in the heart of Inner Mongolia and a significant dust source in Northern China. Additionally, to examine

https://doi.org/10.5194/egusphere-2024-2065
Preprint. Discussion started: 23 August 2024
© Author(s) 2024. CC BY 4.0 License.

the local sources of combined amino acids (CAAs) in $PM_{2.5}$, surface soil samples (0-10 cm) and leaves from the predominant plant, *Platanus orientalis*, were collected in Beijing, Tianjin, Shijiazhuang, and Taiyuan.

2.2 Analyses of the concentration and $\delta^{15}N$ value of CAAs

Extraction methods for combined amino acids (CAAs) in $PM_{2.5}$ were detailed in our previous study (Zhu et al., 2020b). To convert all amino acids to free amino acids, a hydrolysis method was employed. The CAA concentrations were determined by subtracting free amino acid concentrations from total amino acid concentrations. Briefly, one-sixteenth of each filter sample (~80 m^3 of air) was cut into small pieces and hydrolyzed using 10 mL of 6 M hydrochloric acid at 110°C for 24 h. α-Aminobutyric acid was added as an internal reference. To prevent oxidation, 25 μL of 20 μg μL^{-1} ascorbic acid (500 μg absolute) was added to each filter sample, and each hydrolysis tube was flushed with nitrogen and tightly sealed before hydrolysis. The hydrolyzed solution was cooled, dried under a stream of nitrogen, and then redissolved in 0.1 N HCl (v/v). The extracts of total amino acids were then purified using a cation exchange column (Dowex 50W X $8H^+$, 200-400 mesh; Sigma–Aldrich, St Louis, MO, USA), eluted with 10 mL of 10% aqueous ammonia, and dried under nitrogen. Finally, tert-butyldimethylsilyl derivatives of total amino acids were prepared as described in Zhu et al. (2018).

Free amino acids were extracted following the procedure outlined in Zhu et al. (2020b), where one-quarter of each filter sample (~300 m^3 of air) was processed in a Nalgene tube with α-aminobutyric acid as the internal standard and ultrasonically extracted in ice-cold Milli-Q water. The extract underwent ultrasonication, shaking, centrifugation, and filtration through a 0.22 μm cellulose acetate membrane, followed by lyophilization and resuspension in 1 mL of 0.1 N HCl (v/v). The samples were then processed using the same purification and derivatization steps as the total amino acids. Field blank filters were also taken and treated using the same procedure, and all reported values were corrected for blanks. Plant and soil samples were ground separately in liquid nitrogen into fine powders using a mortar and pestle. Then, well ground and homogenized soil and plant power were hydrolyzed, purification and derivatization in the same way as the aerosol samples. For more details refer to our previous publication (Zhu et al., 2021).

https://doi.org/10.5194/egusphere-2024-2065
Preprint. Discussion started: 23 August 2024
© Author(s) 2024. CC BY 4.0 License.

The concentrations of CAAs were analyzed using a gas chromatograph–mass spectrometer (GC–MS). The GC–MS instrument was composed of a Thermo Scientific TRACE GC (Thermo Scientific, Bremen, Germany) connected to a Thermo Scientific ISQ QD single quadrupole MS. More details on instrument conditions, quality assurance and control (including recoveries, linearity, detection limits and quantitation limits) of CAAs are provided in our previous publications (Zhu et al., 2018; Zhu et al., 2020b).

The $\delta^{15}N$ values of AA-tert-butyldimethylsilyl derivatives were analyzed using a Thermo Trace GC (Thermo Scientific, Bremen, Germany) and a conflo IV interface (Thermo Scientific, Bremen, Germany) interfaced with an isotope ratio mass spectrometry (IRMS, Thermo Delta V IRMS, Thermo Scientific, Bremen, Germany). The internal standard with a known $\delta^{15}N$ value (α-aminobutyric acid, -8.17‰ ± 0.03‰) in each sample was checked to determine the reproducibility of the isotope measurements. The analytical run was accepted when the differences between the $\delta^{15}N$ values of α-aminobutyric acid measured by GC-IRMS and its true values were at most 1.5 ‰. The analytical precisions (SD, n=9) of the $\delta^{15}N$ measurements for derivatized amino acid standards ranged from 0.5‰ to 1.4‰. The difference between amino acid $\delta^{15}N$ values measured by using an elemental analysis/IRMS (EA/IRMS) and GC/MS/IRMS after empirical correction ranged from 0.1‰ to 1.3‰. Each reported value is the mean of at least three $\delta^{15}N$ determinations. The detailed instrument conditions and method validation were described in our previous study (Zhu et al., 2018; Zhu et al., 2020b). Since asparagine and glutamine are converted to aspartic acid and glutamic acid in the hydrolysis process, respectively, the concentrations and $\delta^{15}N$ values of combined asparagine and glutamine could not be determined by this method. The concentration and $\delta^{15}N$ value of combined aspartic acid represents the sum of aspartic acid and asparagine. The concentration and $\delta^{15}N$ value of combined glutamic acid represents the sum of glutamic acid and glutamine.

2.3 Analysis of the dry deposition fluxes

In this study, the atmospheric deposition fluxes of CAAs (mg N m^{-2} d^{-1}) at four sampling sites are estimated from equation 1:

$$F_{dry}=C\cdot V_d \quad (1)$$

https://doi.org/10.5194/egusphere-2024-2065
Preprint. Discussion started: 23 August 2024
© Author(s) 2024. CC BY 4.0 License.

where C is the atmospheric concentration (nmol N m^{-3}) and Vd is the dry deposition velocity (m s^{-1}). Vd is controlled by the aerosol size, wind speed, aerosol hygroscopicity, relative humidity and underlying surface. The average deposition velocity of CAAs was 0.012 m s^{-1}, which has also been widely used to estimate water-soluble organic nitrogen (WSON) dry deposition (Zamora et al., 2011). However, actual Vd values were poorly quantified. The dry deposition flux may be under- or overestimated by using a fixed deposition velocity (Luo et al., 2018; Zamora et al., 2011).

A "new" input of CAA-N (protein-N) supplied by the Gobi Desert for the ecosystems in the downwind region (Input Fdry) can be calculated from equation 2:

$$\text{Input Fdry} = \text{Fdry} \cdot f \quad (2)$$

where Fdry is the atmospheric deposition fluxes of protein-N, which is calculated from equation 1.f is the contribution of the Gobi dust source at each sampling site, which is obtained from the nitrogen isotopic mass balance (equation 3).

$$\delta^{15}N_{AA\ during\ the\ dust\ period} = \delta^{15}N_{AA\ during\ the\ non\text{-}dust\ period} \cdot (1-f) + \delta^{15}N_{AA\ dust\ source} \cdot f \quad (3)$$

where $\delta^{15}N_{AA\ during\ the\ dust\ period}$ is $\delta^{15}N$ value of the specific amino acid measured during the dust period, $\delta^{15}N_{AA\ during\ the\ non\text{-}dust\ period}$ is $\delta^{15}N$ value of the specific amino acid measured during the non-dust period and $\delta^{15}N_{AA\ dust\ source}$ is $\delta^{15}N$ value of the specific amino acid measured in the Gobi dust source. f is the contribution of the Gobi dust source at each sampling site.

2.4 Auxiliary Data

The meteorological data during the sampling period were collected from the Global Weather and Climate Information Network (http://www.weatherandclimate.info/). The MODIS satellite images were available at the following website: https://worldview.earthdata.nasa.gov/.

2.5 Statistics

Statistical analysis was conducted by Origin 2018 (OriginLab Corporation, USA). We performed a one-way analysis of variance (ANOVA) for the concentrations of PM_{10}, the ratios of Ala%/Pro%, Gly%/Pro% and Glu%/Pro%, $\delta^{15}N$ values of Glycine and leucine, testing the effect of dust storms. Tukey's honestly significant difference (Tukey-HSD) test was used to compare the significant difference. Further, the differences in the $\delta^{15}N$ values of combined glycine leucine, isoleucine, alanine and valine in $PM_{2.5}$ at four cities during the non-dust period and their corresponding values in the surface soil in the Gobi Desert

https://doi.org/10.5194/egusphere-2024-2065
Preprint. Discussion started: 23 August 2024
© Author(s) 2024. CC BY 4.0 License.

were examined using the one-way ANOVA procedure and compared using the Tukey-HSD test. For all tests, statistically significant differences were considered at $p < 0.05$.

3 Results

3.1 Concentrations of $PM_{2.5}$ and PM_{10} in Northern China

Figure 1 illustrated the variations in atmospheric $PM_{2.5}$ and PM_{10} concentrations across Beijing (BJ), Tianjin (TJ), Shijiazhuang (SJZ), and Taiyuan (TY) throughout the sampling period. Periods when mass concentrations of PM_{10} exceeded 500 μg m^{-3} were as follows: in Beijing from 06:00 to 19:00 on March 28; in Tianjin from 09:00 to 13:00 on the same day; in Shijiazhuang from 11:00 to 18:00; and in Taiyuan from 21:00 on March 28 to 03:00 on March 29, as indicated by a yellow shadow in Figure 1. A MODIS satellite image from NASA (https://worldview.earthdata.nasa.gov/) revealed a dust episode on March 28, 2018, with brown dust plumes visibly overlaying the North China Plain, and significant dust presence persisting on March 29, suggesting that the dust particles did not settle. Consequently, the filter samples from March 28 and 29 were categorized as the dust period, highlighted in yellow in Figure 1. The remaining days of the sampling period were classified as the non-dust period.

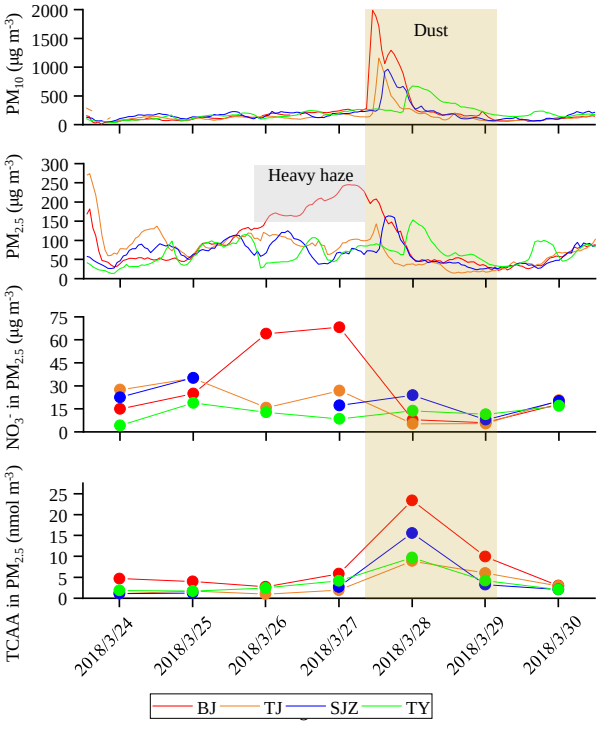

https://doi.org/10.5194/egusphere-2024-2065
Preprint. Discussion started: 23 August 2024
© Author(s) 2024. CC BY 4.0 License.

Figure 1. Time series of $PM_{2.5}$ and PM_{10} concentration, as well as NO_3^-, total combined amino acids (TCAA) in $PM_{2.5}$ at Beijing (BJ), Tianjin (TJ), Shijiazhuang (SJZ) and Taiyuan (TY) from March 24 to March 30, 2018. The yellow shadow indicates the dust period. The grey shadow denotes a heavy haze period in BJ.

As shown in Figure 1, compared to the non-dust period, the concentrations of PM_{10} during the dust period exhibited a significant increase at four sampling sites, by factors of 8.7 in Beijing, 6.3 in Tianjin, 4.8 in Shijiazhuang, and 3.2 in Taiyuan ($p < 0.01$). Among four sampling sites, Beijing recorded the highest increase in PM_{10} concentration with the peak value of 1989 μg m^{-3} on 28 March (Figure 1). In comparison to PM_{10}, the increase in $PM_{2.5}$ concentration during the dust period was less pronounced. Beijing experienced a severe haze event two days before the dust invasion (March 26 and 27), with $PM_{2.5}$ concentrations surpassing 150 μg m^{-3}. Following the dust invasion, Beijing's $PM_{2.5}$ rapidly dropped to 50 μg m^{-3} by 23:00 on March 28. In Tianjin, the $PM_{2.5}$ concentration first increased and peaked at 143 μg m^{-3} at 08:00 on March 28 (dusty day). Subsequently, similar to Beijing, Tianjin's $PM_{2.5}$ rapidly decreased to 36 μg m^{-3}. Contrast to Beijing and Tianjin, $PM_{2.5}$ in Shijiazhuang and Taiyuan, showed an upward trend following the dust invasion, with daily averages rising from 62 and 78 μg m^{-3} on March 27 to 79 and 94 μg m^{-3} on March 28, respectively. Overall, there was a decrease in the $PM_{2.5}/PM_{10}$ ratio at all locations. This ratio declined from 0.7 to 0.1 in Beijing, 0.6 to 0.1 in Tianjin, 0.4 to 0.2 in Shijiazhuang, and 0.4 to 0.2 in Taiyuan (Table S1), further indicating a significant increase in coarse particulate matter due to the dust storms.

The 48-h backward trajectories and clusters of air mass trajectories at the four sampling sites on March 28th, 2018 are displayed in Figure 2. The air masses arriving at the four sampling sites during the dust period primarily originated from the Gobi Desert. Observation from the MODIS satellite also confirmed that the occurrences of dust storm events across four sampling sites originated from the Gobi Desert (Figure S1).

https://doi.org/10.5194/egusphere-2024-2065
Preprint. Discussion started: 23 August 2024
© Author(s) 2024. CC BY 4.0 License.

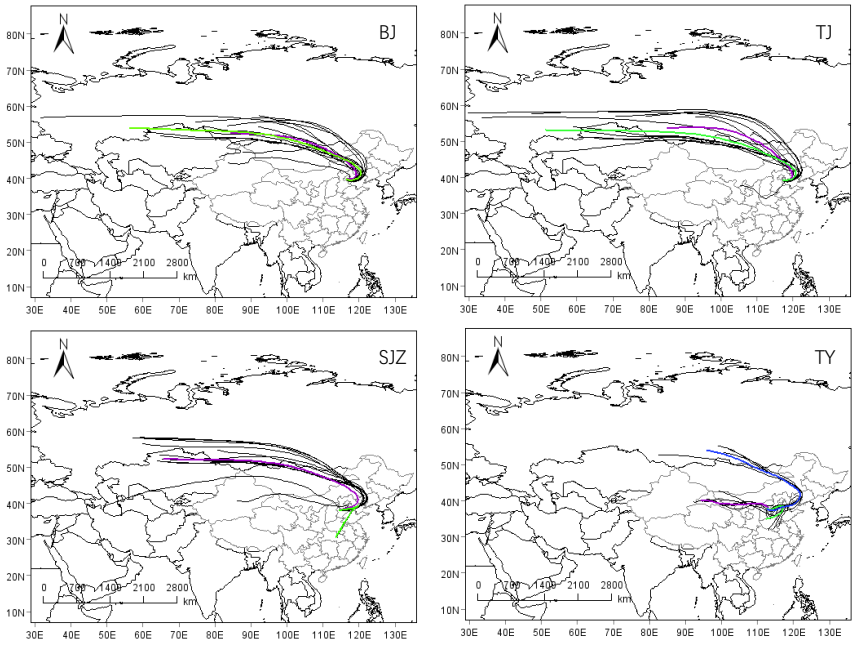

Figure 2. 48h backward trajectories of air masses arriving in reaching Beijing, Tianjin, Shijiazhuang and Taiyuan at 500m above ground level during the dust period. Color lines show the cluster results of air mass trajectories. Trajectories were divided into two or three clusters in four cities. The main contribution clusters in these cities were found to be primarily originated from the Gobi Desert.

3.2 Concentrations and distribution of CAAs

3.2.1 CAAs in the Gobi Desert sources

Given that this dust storm originated from the Gobi Desert (Figure 3), we investigated the molar composition of CAAs in both the surface soils and dominant plants of the region to determine the characteristic molar percentages of proteins transported from the Gobi Desert. In the surface soil of the Gobi Desert, glycine and alanine were the most abundant combined amino acids, each contributing approximately 20.4 ± 5.6% and 20.7 ± 2.9%, respectively, to the total CAAs pool (Figure 3a). Glutamic acid was the predominant CAA species in typical Gobi plants, accounting for 21.0%, 22.5%, and 69.3% of the total CAAs pool in *chenopodium ambrosioides*, *Tripogon chinensis*, and *tamarix chinensis*, respectively (Figure 3a).

https://doi.org/10.5194/egusphere-2024-2065
Preprint. Discussion started: 23 August 2024
© Author(s) 2024. CC BY 4.0 License.

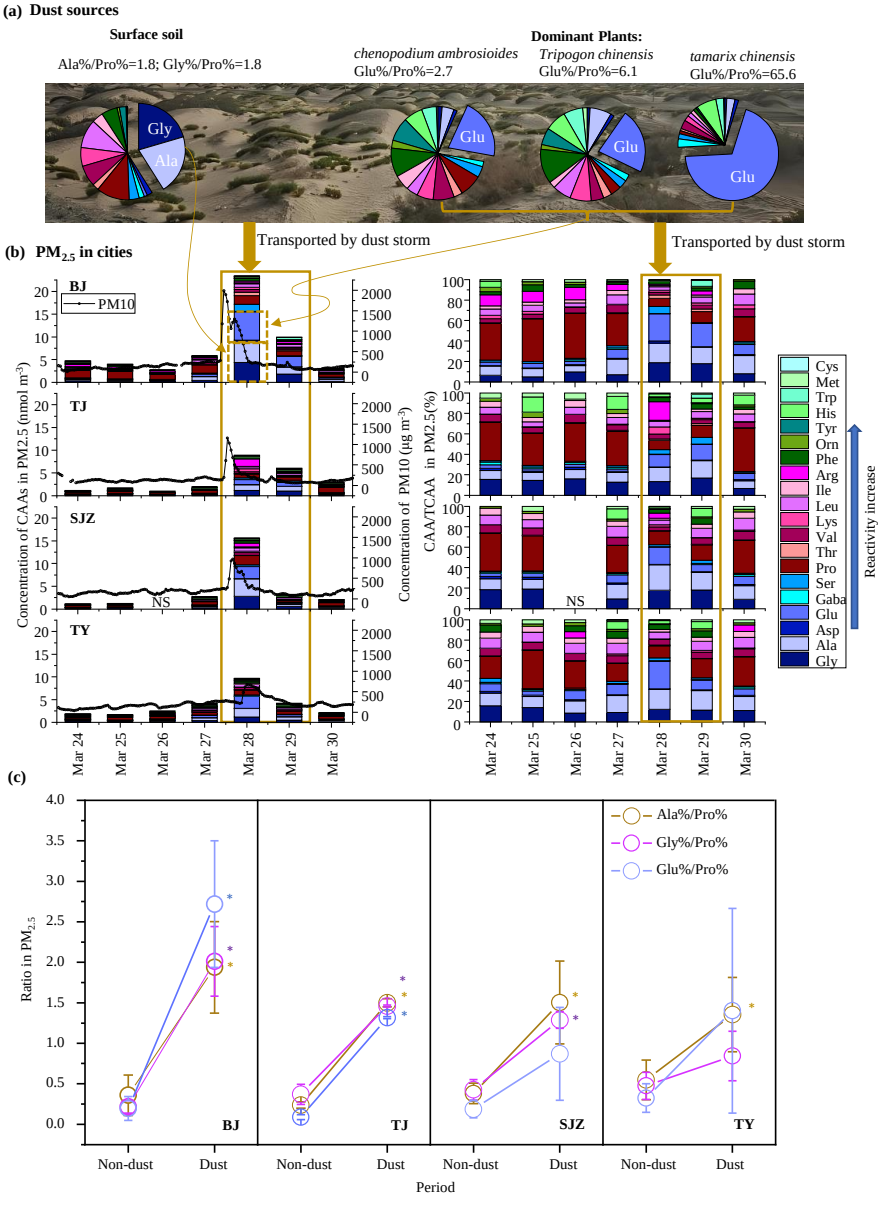

Figure 3. (a) The percent distributions of each individual CAAs (% of total CAAs) in the surface soils and three dominant plants (*chenopodium ambrosioides*, *Tripogon chinensis*, and *tamarix chinensis*) in the Gobi Desert. (b) Concentrations and distribution of individual CAAs at BJ, TJ, SJZ and TY. (c) the average ratios of the percentage of alanine, glycine, and glutamic acid to proline (Ala%/Pro%, Gly%/Pro%, Glu%/Pro%) in $PM_{2.5}$ on dusty and non-dust days at four cities. Asterisks indicate a significant difference in the average ratio between dust and non-dust periods (one-way ANOVA, $p < 0.05$).

https://doi.org/10.5194/egusphere-2024-2065
Preprint. Discussion started: 23 August 2024
© Author(s) 2024. CC BY 4.0 License.

In both the surface soil and common plants of the Gobi Desert, the molar percentage of combined proline was lower than those of the amino acids mentioned earlier, contributing only 11.4 ± 3.3% to the total CAAs pool of the Gobi surface soil. Among the three common plants, the molar percentage of proline did not exceed 8%. Therefore, the proteins transported from Gobi Desert are predominantly composed of alanine, glycine, and glutamic acid (Figure 3a).

3.2.2 Total CAAs concentration in $PM_{2.5}$ in Northern China

The temporal variations of total CAAs in $PM_{2.5}$ measured at all sites during the sampling period were shown in Figure 1. A marked increment in the total CAAs in fine particles were observed at all sampling locations. The average concentrations of total CAAs in $PM_{2.5}$ in Beijing, Tianjin, Shijiazhuang, and Taiyuan increased from the non-dust period of 4.0, 1.7, 1.8, and 2.5 nmol m^{-3} to 16.7, 7.5, 9.4, and 6.9 nmol m^{-3} during the dust period, respectively ($p < 0.01$). The temporal variation of the total CAAs concentration were consistent with that of PM_{10} at four cities (Figure 1). The highest concentrations of total CAAs at four sites occurred on 28 March 2018 coincided with peaks in the enrichment of PM_{10} concentrations.

As exhibited in Figure 1, the temporal variation pattern of NO_3^- concentration in $PM_{2.5}$ was similar to that of $PM_{2.5}$, which was quite different from that of total CAAs concentrations in $PM_{2.5}$ at Beijing and Tianjin. At Beijing and Tianjin, the highest concentration of NO_3^- in $PM_{2.5}$ occurred on 27 March (non-dust day), but decreased on 28 March and 29 March (dust day). The difference in the temporal variations of total CAAs and NO_3^- in $PM_{2.5}$ may point to the contribution of different sources during the sampling period.

3.2.3 Individual CAAs in $PM_{2.5}$ in Northern China

For individual amino acid species in $PM_{2.5}$, the concentrations of alanine and glycine, which predominate in the surface soil of the Gobi Desert, increased markedly during the dust period (Figure 3b). Specifically, alanine concentrations in $PM_{2.5}$ during the dust period were 3.0 ± 2.0, 1.1 ± 0.2, 2.2 ± 2.3 and 1.3 ± 0.8 nmol m^{-3} at Beijing, Tianjin, Shijiazhuang, and Taiyuan, being 7, 8, 10 and 4 times more than that during the non-dust period, respectively. Glycine concentrations in $PM_{2.5}$ rose from 0.3 ± 0.1, 0.2 ± 0.04, 0.2 ± 0.03 and 0.3 ± 0.07nmol m^{-3} during the non-dust period to 3.1 ± 1.8, 1.1 ± 0.1, 1.7 ± 1.6 and 0.8 ± 0.5 nmol m^{-3} during the dust period at Beijing, Tianjin, Shijiazhuang and Taiyuan, respectively. Similarly,

https://doi.org/10.5194/egusphere-2024-2065
Preprint. Discussion started: 23 August 2024
© Author(s) 2024. CC BY 4.0 License.

the concentrations of glutamic acid, which predominate in common plants of the Gobi Desert, increased markedly during the dust period, with concentrations 17, 15, 12 and 8 times higher than that of the non-dust period at Beijing, Tianjin, Shijiazhuang and Taiyuan, respectively (Figure 3b). In contrast, the concentrations of other CAAs displayed no significant variation between the dust and non-dust periods. During the dust period, the molar composition of CAAs in $PM_{2.5}$ shifted significantly at all sampling locations, compared to the non-dust period (Figure 3b). In the non-dust period, combined proline dominated the total CAAs pool in $PM_{2.5}$, contributing to 35.4%, 36.3%, 32.3%, and 26.0% in Beijing, Tianjin, Shijiazhuang, and Taiyuan, respectively, as illustrated by the dark red shadow in Figure 2b. This prevalence diminished across all sites during the dust period, with molar percentages of combined proline dropping to 9.4%, 10.3%, 13.9%, and 14.9%, correspondingly. Concurrently, there was a marked increase in the molar percentages of combined alanine, glycine, and glutamic acid (blue shadow in Figure 3b). The average molar percentages of these three CAAs in fine particulates increased from 24.4%, 24.9%, 31.6%, and 31.9%, respectively, during the non-dust period to 61.1%, 44.2%, 50.4%, and 48.8% during the dust period, thus emerging as the dominant CAA species at these locations. Notably, in Beijing, the molar percentage of combined proline exhibited the largest decrease, while the sum of the molar percentage of combined alanine, glycine, and glutamic acid which is abundant in soil and plants of the Gobi Desert, showed the greatest increase.

Based on the variation trends in the percentage composition of CAAs in $PM_{2.5}$ across four cities during the dust and non-dust period, the ratios of the percentage of alanine, glycine, and glutamic acid to proline (Ala%/Pro%, Gly%/Pro%, Glu%/Pro%) in $PM_{2.5}$ on dusty days were compared to those on non-dust days across the four cities. The results showed that in Beijing and Tianjin, the ratios of Ala%/Pro%, Gly%/Pro% and Glu%/Pro% increased significantly on dusty days compared to non-dust days ($p < 0.05$) (Figure 3c). In Shijiazhuang, during the dust period, the ratios of Ala%/Pro% and Gly%/Pro% also showed significant increases relative to non-dust days ($p < 0.05$), whereas in Taiyuan, only the Ala%/Pro% ratio increased significantly during the dust period ($p < 0.05$) (Figure 3c).

https://doi.org/10.5194/egusphere-2024-2065
Preprint. Discussion started: 23 August 2024
© Author(s) 2024. CC BY 4.0 License.

3.3 Compound-specific nitrogen isotopes of CAAs (δ^{15}N-CAAs)

3.3.1 δ^{15}N-CAAs in Gobi Desert

δ^{15}N-CAAs of individual CAAs in the surface soil and predominant plants in the Gobi Desert were compared with those in $PM_{2.5}$ at four urban sites during non-dust period (Figure 4, right side). Glycine, leucine, isoleucine, alanine and valine were ^{15}N-depleted in the Gobi Desert surface soil compared to those in $PM_{2.5}$ at the urban sites during the non-dust period, whereas δ^{15}N values of other individual CAA species were close between these two sources (Figure 4, right side). Among these four CAA species, the most significant δ^{15}N depletion was observed for glycine and leucine. The mean δ^{15}N values of glycine and leucine showed statistically significant differences between the Gobi Desert surface soil and urban $PM_{2.5}$ during the non-dust period (one way ANOVA, $p < 0.01$) (Figure 5). Specifically, glycine and leucine in Gobi Desert surface soil were depleted in ^{15}N by 12 to 14‰ and 6 to 11‰, respectively, relative to their corresponding values in urban $PM_{2.5}$ during the non-dust period (Figure 4, right side, yellow box).

https://doi.org/10.5194/egusphere-2024-2065
Preprint. Discussion started: 23 August 2024
© Author(s) 2024. CC BY 4.0 License.

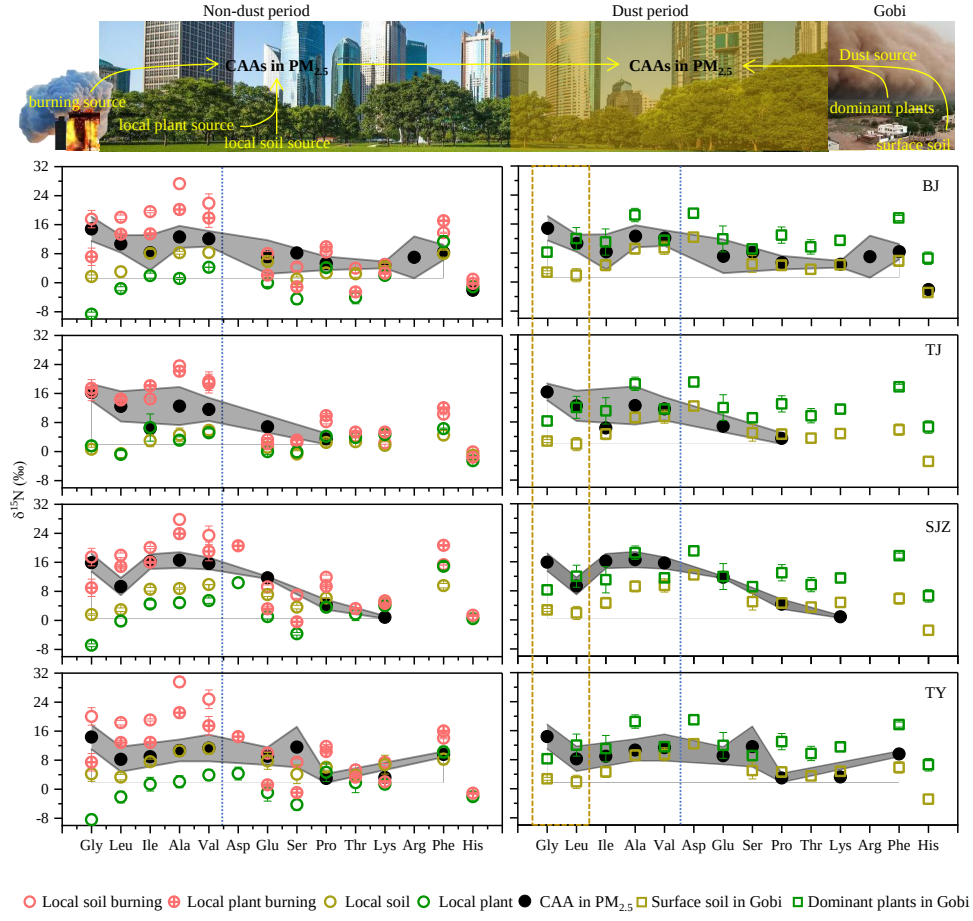

Figure 4. Comparison of δ^{15}N-CAA patterns of in $PM_{2.5}$ at BJ, TJ, SJZ and TY with those in potential local sources and Gobi dust sources. CAAs species on the left side of blue dotted line were ^{15}N-depleted in the Gobi Desert surface soil compared to those in $PM_{2.5}$ at the urban sites during the non-dust period. CAAs species in the yellow dotted box exhibited the most significant δ^{15}N depletion compared to those in $PM_{2.5}$ at the urban sites during the non-dust period.

https://doi.org/10.5194/egusphere-2024-2065
Preprint. Discussion started: 23 August 2024
© Author(s) 2024. CC BY 4.0 License.

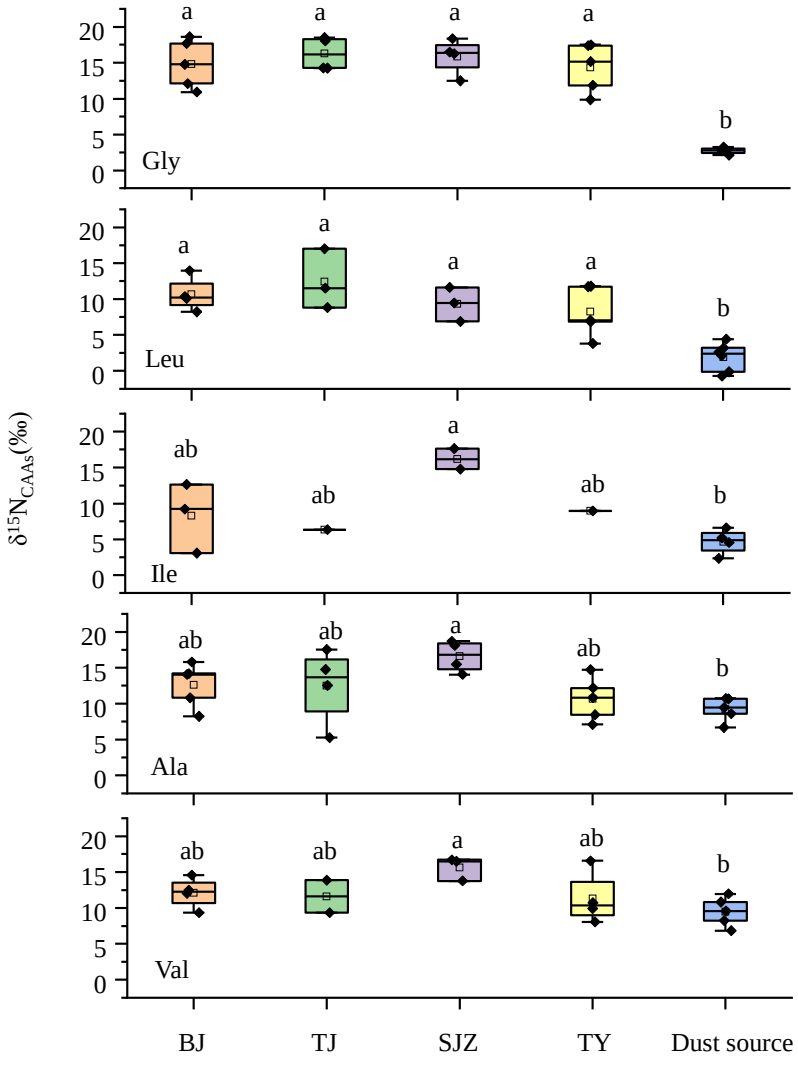

Figure 5. The $\delta^{15}N$ values of combined glycine (Gly), leucine (Leu), isoleucine (Ile), alanine (Ala) and valine (Val) in $PM_{2.5}$ at Beijing (BJ), Tianjin (TJ), Shijiazhuang (SJZ) and Taiyuan (TY) during the non-dust period and their corresponding values in the surface soil in the Gobi Desert. Different lower-case letter denote means found to be statistically different (one-way ANOVA, $p < 0.05$).

Compared to the surface soil of the Gobi Desert, predominant plants in the region exhibited significant ^{15}N enrichments of 2–12‰ for all CAA species (Figure 4, right side, green box). It is noteworthy that the average $\delta^{15}N$ value of combined glutamic acid (11.9 ± 3.6‰), the predominant amino acid in these plants,

https://doi.org/10.5194/egusphere-2024-2065
Preprint. Discussion started: 23 August 2024
© Author(s) 2024. CC BY 4.0 License.

was close to its values in urban $PM_{2.5}$ during the non-dust period at four cities (one-way ANOVA, $p > 0.05$).

3.3.2 δ^{15}N-CAAs in $PM_{2.5}$ in Northern China

Figure 4 shows the δ^{15}N patterns of individual CAAs in $PM_{2.5}$ (dark circle), local common plant (green circle) and local soil (yellow circle) as well as local burning sources (pink circle) from four urban sites. During the non-dust period, δ^{15}N-CAAs patterns in $PM_{2.5}$ at four urban sites were generally consistent, with glycine, leucine, isoleucine, alanine and valine exhibiting relatively higher δ^{15}N values than other CAA species (Figure 4, left side). Besides that, δ^{15}N values of individual CAAs in $PM_{2.5}$ all fell within their respective ranges observed in local dominant plants, soil, and burning sources at four cities (Figure 4, left side).

During the dust period, glycine, alanine, valine, leucine, and isoleucine showed negative shifts in δ^{15}N values compared to those observed during the non-dust periods (Figure 6). In contrast, the δ^{15}N shifts in other CAA species between the dust and non-dust periods were either relatively minimal or displayed δ^{15}N enrichments (Figure 6). A spatial variation in δ^{15}N depletions for these five amino acids was observed, with the largest depletions occurring in Beijing. The degree of δ^{15}N-CAA shifts decreased in the order of Beijing, Tianjin, Shijiazhuang, and Taiyuan. In Taiyuan, the δ^{15}N shifts in all five amino acids during the dust period were not observed.

https://doi.org/10.5194/egusphere-2024-2065
Preprint. Discussion started: 23 August 2024
© Author(s) 2024. CC BY 4.0 License.

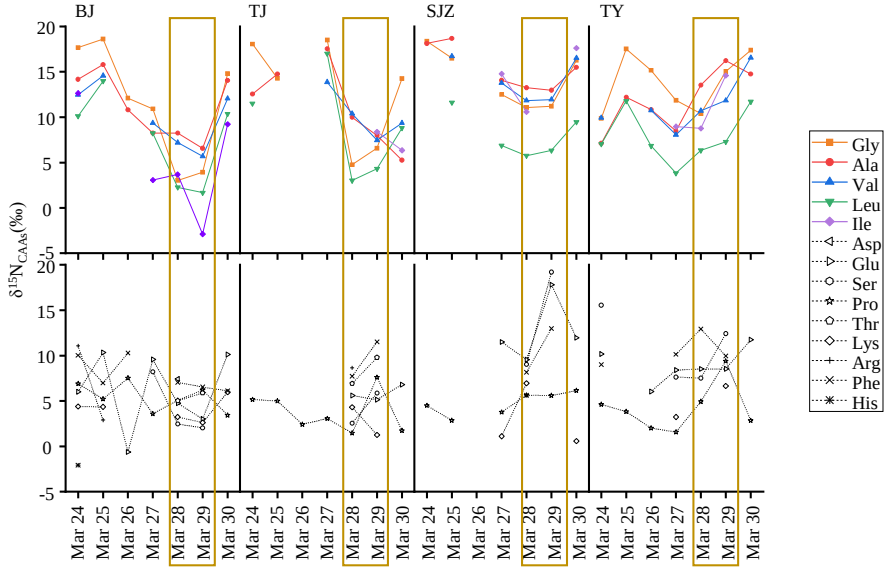

Figure 6. Time series of $\delta^{15}N$ of individual CAAs in $PM_{2.5}$ at BJ, TJ, SJZ and TY. The yellow box represents the dust period.

Among these five amino acids, glycine and leucine in $PM_{2.5}$ exhibited the most significant $\delta^{15}N$ depletion during the dust period at four sampling sites (Figure 6). The $\delta^{15}N$ values of combined glycine in $PM_{2.5}$ significantly decreased from 14.8‰, 16.3‰, and 15.9‰ during the non-dust period to 3.5‰, 5.7‰ and 11.1‰, respectively, during the dust period at Beijing, Tianjin and Shijiazhuang (one-way ANOVA, $p < 0.05$) (Figure 7a). At Taiyuan, the average $\delta^{15}N$ values of combined glycine in $PM_{2.5}$ during the non-dust (14.4‰) and dust period (12.7‰) were not significantly different ($p > 0.05$). Remarkably, the $\delta^{15}N$ values of combined glycine in Beijing's $PM_{2.5}$ during the dust period ranged from 3.0‰ to 3.9‰, closely aligning with those found in surface soils of the Gobi Desert, which ranged from +2.1‰ to +3.2‰ (Figure 7a). Similarly, the $\delta^{15}N$ values of combined leucine in $PM_{2.5}$ from Beijing and Tianjin sharply decreased from +10.7‰ and +12.4‰ during the non-dust period to +2.0‰ and +3.7‰, respectively, during the dust period (one-way ANOVA, $p < 0.05$) (Figure 7b). At Shijiazhuang and Taiyuan, there was no significant variation in the mean $\delta^{15}N$ values of leucine between the non-dust and dust period ($p>0.05$) (Figure 7b).

https://doi.org/10.5194/egusphere-2024-2065
Preprint. Discussion started: 23 August 2024
© Author(s) 2024. CC BY 4.0 License.

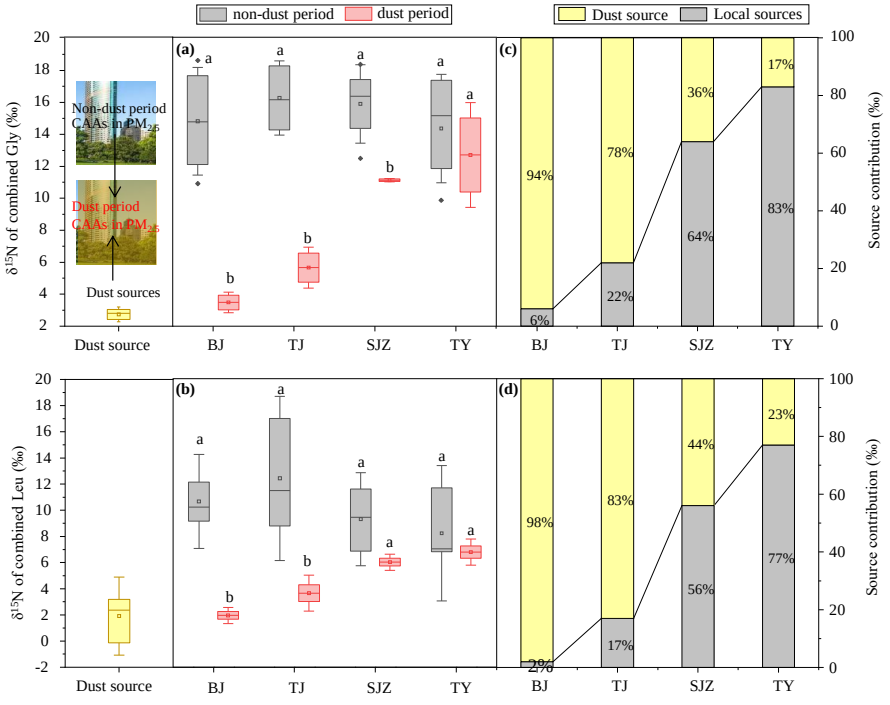

Figure 7. (a) $\delta^{15}N$ values of combined glycine in surface soil from Gobi Desert (yellow box) and in $PM_{2.5}$ during the non-dust (grey box) and dust (red box) period at Beijing, Tianjin, Shijiazhuang and Taiyuan; (b) $\delta^{15}N$ values of combined leucine in surface soil from Gobi Desert (yellow box) and in $PM_{2.5}$ during the non-dust (grey box) and dust (red box) period; (c) the contribution of Gobi dust sources and local urban sources to the CAAs in $PM_{2.5}$ calculated by the nitrogen isotopic mass balance for glycine; (d) the contribution of Gobi dust sources and local urban sources to the CAAs in $PM_{2.5}$ calculated by the nitrogen isotopic mass balance for leucine. Different lower-case letter denote means found to be statistically different (one-way ANOVA, $p < 0.05$) between the non-dust and dust period.

Moreover, as mentioned above, one-way ANOVA revealed significant differences in the $\delta^{15}N$ values of glycine and leucine between Gobi Desert surface soil and urban $PM_{2.5}$ during the non-dust period ($p<0.01$; Figure 5). Therefore, a simple nitrogen isotopic mass balance was employed to estimate the contribution of long-range transported Gobi dust sources to proteinaceous matter in $PM_{2.5}$ at four cities. The results of the nitrogen isotopic mass balance for both glycine and leucine were consistent. During the dust period, long-range transported Gobi dust sources contributed 94~98%, 78~83%, 36~44% and 17~23% to proteinaceous matter in $PM_{2.5}$ at Beijing, Tianjin, Shijiazhuang and Taiyuan, respectively (Figure 7c and d).

https://doi.org/10.5194/egusphere-2024-2065
Preprint. Discussion started: 23 August 2024
© Author(s) 2024. CC BY 4.0 License.

3.4 Dry deposition fluxes of protein-N

A "new" input of CAA-N (protein-N) supplied by the Gobi Desert for the ecosystems in the downwind region were calculated from equation 2. The contribution of the Gobi dust source at each sampling site (f) was obtained from the nitrogen isotopic mass balance (Figure 7c and d). The average dry deposition of protein-N collected at each site during the non-dust period served as the background levels. The dry deposition flux of protein-N in $PM_{2.5}$ sharply increased from the non-dust to the dust period at all four sampling sites. During the dust period, the dry deposition of protein-N (Fdry) in $PM_{2.5}$ was 0.37, 0.22, 0.28, and 0.15 mg N m^{-2} d^{-1} in Beijing, Tianjin, Shijiazhuang and Taiyuan, respectively. The input of protein-N from the Gobi dust (Input Fdry) was approximately 4.5, 6.3, 3.3, and 1.3 times higher than the background levels in Beijing, Tianjin, Shijiazhuang, and Taiyuan, respectively (Figure 8).

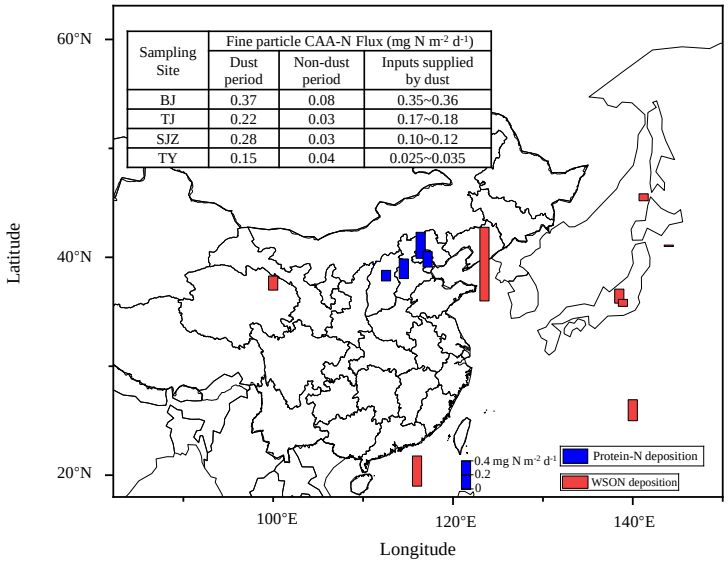

Figure 8. The dry deposition flux of protein-N at BJ, TJ, SJZ and TY during the dust period (blue bar) and published reports of the dry deposition flux of WSON measured in different atmospheric scenarios (red bar). The length of the bars represents the dry deposition flux of WSON and protein-N. The WSON deposition data were sourced from previous studies (Shi et al., 2010; Ho et al., 2015; Matsumoto et al., 2014; Tsagkaraki et al., 2021; Nakamura et al., 2006; Zhang et al., 2011).

https://doi.org/10.5194/egusphere-2024-2065
Preprint. Discussion started: 23 August 2024
© Author(s) 2024. CC BY 4.0 License.

4 Discussion

4.1 Source identification of CAAs in urban $PM_{2.5}$

Amino acids constitute a major component of water-soluble organic nitrogen and play significant roles in biological activities. Previous studies focused on the levels and distribution of free amino acids in urban aerosols during the dust period (Mace et al., 2003; Shi et al., 2010), revealing that free amino acids typically represent a minor portion of the organic nitrogen, accounting for approximately 1% of the total organic nitrogen, with no significant increase in their average concentrations during dust periods. However, CAAs are the predominant form of the amino acid compounds in aerosols, with concentrations approximately five times higher than those of FAAs (Matsumoto et al., 2021; Wedyan and Preston, 2008). Furthermore, recent studies have suggested that microbial communities in desert soils might travel long distances via desert dust (Favet et al., 2013; Petroselli et al., 2021). Proteins (CAAs) are significant components of these microbes. Therefore, it is reasonable to hypothesize that during the dust period, the proteinaceous matter in desert could be one of the potential sources of CAAs in aerosols in downwind cities.

This study presents the first simultaneous measurements of the levels and distribution of CAAs in $PM_{2.5}$ across four urban areas during a dust event. The concentrations of total CAAs in $PM_{2.5}$ increased sharply at all sampling sites during the dust period ($p < 0.01$) (Figure 1). Furthermore, the temporal variation pattern of total CAAs in $PM_{2.5}$ was consistent with that of PM_{10} (Figure 1). An increase in PM_{10} indicates a rise in dust coarse particle levels (Wu et al., 2019). Synchronous changes between the total CAAs and PM_{10} during the dust period suggested the increase concentration of CAAs in $PM_{2.5}$ during the dust period were directedly linked to the long-transported Gobi dust source. Conversely, the concentration of total CAAs displayed an inverse temporal variation pattern with nitrate (NO_3^-) concentration (Figure 1). In contrast, NO_3^- is a key component of secondary inorganic aerosols in $PM_{2.5}$, which formed via photochemical oxidation reactions of NOx (Song et al., 2021). Previous studies demonstrated that local urban coal combustion, vehicle exhausts, biomass burning, and microbial N cycle was the major contributor to the atmospheric NO_3^- in Beijing (Song et al., 2019; Zhang et al., 2021). Therefore, decreasing trend of NO_3^- concentration in Beijing and Tianjin during the dust period suggested the lower contribution of local urban sources to CAAs in $PM_{2.5}$ at these two cities during the dust period.

https://doi.org/10.5194/egusphere-2024-2065
Preprint. Discussion started: 23 August 2024
© Author(s) 2024. CC BY 4.0 License.

The compositional profiles of CAAs in aerosols have been utilized to identify the sources of primary aerosol particles (Abe et al., 2016; Matsumoto et al., 2021). This study found a prevalent concentration of combined proline in the total CAAs pool of $PM_{2.5}$ across all sites during the non-dust period, likely due to proline being the major CAA species in urban plants and spores (Barbaro et al., 2015; Matsumoto et al., 2021; Zhu et al., 2020b). The sampling occurred in spring, a period marked by rapid growth of plants and spore emissions. During the dust period, the distribution profiles of CAAs in $PM_{2.5}$ at all observation sites changed, exhibiting consistent variation patterns. Notably, there was a significant increase in the proportions of combined glycine, alanine and glutamic acid, the most abundant amino acids in surface soil and predominant plants from the Gobi Desert (Figure 3). Moreover, substantial amounts of alanine, glycine and glutamic acid from Gobi Desert surface soil and plants into $PM_{2.5}$ in downwind areas led to increased ratios of Ala%/Pro%, Gly%/Pro%, and Glu%/Pro% in $PM_{2.5}$ at four cities on dusty days (Figure 2). These findings further support the hypothesis that long transported surface soil and plants from the Gobi Desert significantly contribute to the proteinaceous matter in $PM_{2.5}$ in downwind areas during the dust period.

The $\delta^{15}N$ values of specific amino acid have been utilized as a novel method to identify the sources of amino acids (Batista et al., 2014; Mccarthy et al., 2013; Zhu et al., 2021). The shift in $\delta^{15}N$ values of specific CAAs in urban $PM_{2.5}$ during the dust period may be attributed to the inputs from long-range transport amino acid sources. Combined glycine constitutes a high proportion of the total CAAs pool in the surface soil of the Gobi Desert (averaging 20.4%), while its content is extremely low in common Gobi plants (averaging 1.1%) (Figure 3). Therefore, during dust periods, the $\delta^{15}N$ values of glycine in $PM_{2.5}$ in downwind cities are primarily influenced by the $\delta^{15}N$ values of glycine in the surface soil of the Gobi Desert, rather than by those in Gobi plants. Since the mean $\delta^{15}N$ values of glycine in Gobi Desert surface soil was more negative than that of urban $PM_{2.5}$ during the non-dust period, the mean $\delta^{15}N$ values of glycine in $PM_{2.5}$ from cities impacted by Gobi dust sources would more negative. Leucine is present in roughly equal amounts in both the surface soil and the common plants of the Gobi Desert (averaging about 5.5% each) (Figure 3). The $\delta^{15}N$ values of leucine in predominant plants do not significantly differ from those in $PM_{2.5}$ during the non-dust period, while $\delta^{15}N$ values of leucine in surface soil were significantly lower (Figure 4). Similar to glycine, during dust periods, the $\delta^{15}N$ values of leucine in $PM_{2.5}$ in downwind cities are also primarily influenced by the $\delta^{15}N$ values of leucine in the surface soil of the

https://doi.org/10.5194/egusphere-2024-2065
Preprint. Discussion started: 23 August 2024
© Author(s) 2024. CC BY 4.0 License.

Gobi Desert. Therefore, the ^{15}N depletion of glycine and leucine in urban $PM_{2.5}$ indicated the contribution of Gobi dust source (Figure 5 and 7).

Combining the correlation between combined amino acids and PM_{10}, the variation in the distribution of the CAAs as well as the shift of the $\delta^{15}N$ values of individual amino acids in $PM_{2.5}$ during the dust period, we can conclude that surface soil and predominant plants in the Gobi Desert are substantial contributors of combined amino acid in fine particles in Northern China during the dust period.

4.2 Contribution of dust sources to the CAAs in $PM_{2.5}$ at each city

It is crucial to quantifying the contribution of dust sources to the CAAs in atmospheric $PM_{2.5}$ in different downwind regions. Although all four cities were affected by the same dust source (the Gobi Desert) during this dust event, the extent of increase in CAAs concentrations, the percentage increase in CAA species that are abundant in the Gobi Desert source (Ala%, Gly%, and Glu%), and the degree of $\delta^{15}N$ depletion in glycine and leucine varied among the four sampling sites (Figures 3 and 5). Notably, in Beijing, the increase in concentration and percentage of alanine, glycine, and leucine, as well as the degree of $\delta^{15}N$ depletion in glycine and leucine, were the most significant. These results suggested that the contribution of dust sources to the CAAs in atmospheric $PM_{2.5}$ was different among four sites and Beijing was most strongly affected by the Gobi dust sources.

This study represents the isotopic interpretation of individual CAAs in $PM_{2.5}$ during the dust period to estimate the contribution of dust sources to CAAs in $PM_{2.5}$ in Northern China. According to previous studies, the major sources of atmospheric CAAs include primary biological aerosol particles, soil resuspension and biomass burning (Matsumoto et al., 2021; Song et al., 2017; Zhu et al., 2020b). Therefore, nitrogen isotope values of individual CAAs in the local common plant, surface soil and burning sources were considered in this study. The nitrogen isotope values of individual CAAs from local burning sources were calculated based on the nitrogen isotope values of individual CAAs in local plants and soil, as well as their nitrogen isotopic fractionation during combustion. Our previous study showed that during combustion, the nitrogen isotope values of glycine, leucine, isoleucine, alanine, and valine increased by 15.8‰, 15.0‰, 11.5‰, 19.0‰, and 13.6‰, respectively, compared to their initial values, while other amino acids showed an isotopic increase of less than 5.8‰. Clearly, the combustion process led to significant enrichment of nitrogen isotopes in specific amino acids, with the most

https://doi.org/10.5194/egusphere-2024-2065
Preprint. Discussion started: 23 August 2024
© Author(s) 2024. CC BY 4.0 License.

substantial ^{15}N enrichment observed in glycine, leucine, isoleucine, alanine, and valine. During the non-dust period, the $\delta^{15}N$ values of individual CAA in $PM_{2.5}$ from four cities all fell within their respective ranges in local common plants, soil, and burning sources across the four urban sites (Figure 4). This indicated that local plants, surface soil and burning sources were the major sources of CAAs in $PM_{2.5}$ across Beijing, Tianjin, Shijiazhuang, and Taiyuan during the non-dust period.

As discussed in Section 4.1, significant quantities of proteinaceous matter transported by dust storms are expected to increase the concentrations of combined glycine and leucine in urban $PM_{2.5}$ and decrease their $\delta^{15}N$ values. Greater inputs of proteinaceous matter from dust storms typically result in more negative $\delta^{15}N$ values of combined glycine and leucine in urban $PM_{2.5}$. Particularly in Beijing, $\delta^{15}N$ values of combined glycine and leucine in $PM_{2.5}$ during the dust period were close to those in the surface soil of the Gobi Desert (Figure 7). Therefore, with known concentrations and isotopic values of specific amino acid in $PM_{2.5}$ during the non-dust periods and during the dust period in downwind regions, as well as the isotopic values of these amino acids from the dust source area, it is possible to calculate the contribution of dust sources to the protein in $PM_{2.5}$ in these downwind regions using nitrogen isotope mass balance for the specific amino acid. Using this approach, the contributions of dust sources to Beijing, Tianjin, Shijiazhuang, and Taiyuan during this dust event were calculated for glycine as 94%, 78%, 36%, and 17% respectively. For leucine, the contributions were 98%, 83%, 44%, and 23%, respectively. The contributions estimated through nitrogen isotope mass balance for glycine align with those derived from leucine (Figure 7). This demonstrates that isotopic mass balance based on the $\delta^{15}N$ values of glycine and leucine in $PM_{2.5}$ is an effective tool for assessing the contribution of dust sources to proteinaceous material in downwind regions.

4.3 Implications of the Gobi Desert-supplied protein-N inputs

Proteinaceous matter in the atmosphere has been studied extensively because it can be a utilizable source of nitrogen for plants and microorganisms (Ho et al., 2015; Samy et al., 2013; Zhang and Anastasio, 2003). Nutrients (e.g., protein-N) whipped up from deserts by strong winds can travel long distances, including over remote oceans (Favet et al., 2013; Yang et al., 2021). Previous studies have shown that dust inputs can stimulate phytoplankton metabolism and thereby enhance new production in the ocean (Duarte et al., 2006; Gazeau et al., 2021). The positive correlation of dust events with chlorophyll a

https://doi.org/10.5194/egusphere-2024-2065
Preprint. Discussion started: 23 August 2024
© Author(s) 2024. CC BY 4.0 License.

concentrations, primary production and spring algae blooms in the south Yellow Sea and East China Sea has been well characterized (Tan et al., 2011). Due to the high bioavailability of amino acids-N, it can serve as a source of nutrients for marine ecosystems and greatly contribute to ecological processes in the marginal seas of China via processes such as fertilization of phytoplankton and stimulation of nitrogen fixation (Duarte et al., 2006; Ho et al., 2015).

In this study, the Gobi Desert-supplied protein-N input (0.35~0.36, 0.17~0.18, 0.10~0.12 and 0.025~0.05 mg N m^{-2} d^{-1} in Beijing, Taiyuan, Shijiazhuang and Taiyuan, respectively) (Figure 8) was compared with published reports of the dry deposition flux of WSON measured in different atmospheric scenarios. Gobi Desert-supplied protein-N input was higher than that observed in a suburban site in northern California, U.S.A. (0.04 mg N m^{-2} d^{-1}) (Zhang et al., 2002). Although the Gobi Desert-supplied protein-N input was lower than the dry deposition of WSON measured in urban sites in China and a coastal site in Qingdao, China, it was markedly higher than those previously measured in the remote Pacific Ocean and Atlantic Ocean areas, consistent with or even higher than those observed at the marginal seas of China (e.g., Yellow Sea and South China Sea) and forested, coastal and rural sites of Japan. Nakamura et al. (2006) suggested that WSON transported from East Asia is an important nitrogen component over the East China Sea. Our results showed that Gobi Desert-supplied protein-N inputs were comparable to or even higher than the dry deposition of WSON in the marginal seas of China (Figure 8).

According to East Asian winter monsoon (from October to April) dynamics, a large quantity of protein-N supplied by Gobi dust found in this study can be deposited in a short period of the year and potentially has important effects on the productivity of oligotrophic ecosystems under the influence of the East Asian dust belt, including China, Korea, Japan and the North Pacific.

5 Conclusion

In this study, the composition profiles of combined amino acids in both the surface soils and dominant plants in the Gobi Desert were characterized. Results indicated that the proteins transported with Gobi Desert dust contain large amounts of alanine, glycine and glutamic acid. Therefore, the concentration of these three CAAs significantly increased and ratios of Ala%/Pro%, Gly%/Pro%, and Glu%/Pro% in $PM_{2.5}$ elevated at four cities on dusty days.

https://doi.org/10.5194/egusphere-2024-2065
Preprint. Discussion started: 23 August 2024
© Author(s) 2024. CC BY 4.0 License.

Moreover, $\delta^{15}N$ patterns of CAAs of the surface soil and predominant plants in the Gobi Desert were demonstrated, which were further used to interpretate the source variation in proteinaceous matter in $PM_{2.5}$ at four cities from the non-dust to dust period. The mean $\delta^{15}N$ values of glycine and leucine in the Gobi Desert surface soil were significantly lower than those in urban $PM_{2.5}$ during the non-dust period, which can be used to tracing Gobi dust sources. According to the $\delta^{15}N$ inventories of individual CAAs in potential emission sources, local plants, surface soil and burning sources were the major sources of CAAs in $PM_{2.5}$ at Beijing, Tianjin, Shijiazhuang, and Taiyuan during the non-dust period. During the dust period, more negative $\delta^{15}N$ values of combined glycine and leucine were observed in $PM_{2.5}$ in Northern China, also suggesting inputs of proteinaceous matter from the Gobi Desert.

The contribution of dust sources to the protein in $PM_{2.5}$ in these downwind regions estimated through nitrogen isotope mass balance for glycine align with those derived from leucine, indicating that isotopic mass balance based on the $\delta^{15}N$ values of glycine and leucine is an effective tool for assessing the contribution of dust sources to proteinaceous material in $PM_{2.5}$. The results showed that protein-N supplied by Gobi dust can reach 0.36 mg N m^{-2} d^{-1}. This large quantity of protein-N deposited in a short period of the year and has important effects on the productivity of oligotrophic ecosystems under the influence of the East Asian dust belt.

Competing interests

The contact author has declared that none of the authors has any competing interests.

Acknowledgments

This work was supported by the National Natural Science Foundation of China (Grant Nos. 42363011). We would like to thank the Global Weather and Climate Information Network (http://www.weatherandclimate.info/) for providing meteorological parameters, including temperature (T), relative humidity (RH) and precipitation, during the sampling period. We would also like to thank the China Air Quality Online Monitoring and Analysis Platform for providing air quality data (https://www.aqistudy.cn/) and NASA's EOSDIS Worldview for providing MODIS satellite images (https://worldview.earthdata.nasa.gov/).

https://doi.org/10.5194/egusphere-2024-2065
Preprint. Discussion started: 23 August 2024
© Author(s) 2024. CC BY 4.0 License.

Data Availability Statement

Meteorological parameters, including temperature (T), relative humidity (RH), and windspeed (WD), during the sampling period are available at the following website: http://www.weatherandclimate.info/. Air quality data, including $PM_{2.5}$ and PM_{10} concentrations, are available at the following website: https://www.aqistudy.cn/.

References

Abe, R. Y., Akutsu, Y., and Kagemoto, H.: Protein amino acids as markers for biological sources in urban aerosols, Environmental Chemistry Letters, 14, 155–161, https://doi.org/10.1007/s10311-015-0536-0, 2016.

Barbaro, E., Zangrando, R., Vecchiato, M., Piazza, R., Cairns, W. R. L., Capodaglio, G., Barbante, C., and Gambaro, A.: Free amino acids in Antarctic aerosol: potential markers for the evolution and fate of marine aerosol, Atmospheric Chemistry and Physics, http://www.atmos-chem-phys.net/15/5457/2015/, 2015.

Batista, F. C., Ravelo, A. C., Crusius, J., Casso, M. A., and McCarthy, M. D.: Compound specific amino acid $\delta^{15}N$ in marine sediments: A new approach for studies of the marine nitrogen cycle, Geochimica et Cosmochimica Acta, 142, 553-569, http://www.sciencedirect.com/science/article/pii/S0016703714004979, 2014.

Chan, M. N., Choi, M. Y., Ng, N. L., and Chan, C. K.: Hygroscopicity of Water-Soluble Organic Compounds in Atmospheric Aerosols: Amino Acids and Biomass Burning Derived Organic Species, Environmental Science & Technology, 39, 1555-1562, https://doi.org/10.1021/es049584l, 2005.

Duarte, C. M., Dachs, J., Llabrés, M., Alonso-Laita, P., Gasol, J. M., Tovar-Sánchez, A., Sañudo-Wilhemy, S., and Agustí, S.: Aerosol inputs enhance new production in the subtropical northeast Atlantic, Journal of Geophysical Research: Biogeosciences, 111, https://doi.org/10.1029/2005JG000140, 2006.

Elbert, W., Taylor, P. E., Andreae, M. O., and Pöschl, U.: Contribution of fungi to primary biogenic aerosols in the atmosphere: active discharge of spores, carbohydrates, and inorganic ions by Asco- and Basidiomycota, Atmospheric Chemistry and Physics Discussions, 6, 11317-11355, https://hal.archives-ouvertes.fr/hal-00302269, 2007.

Favet, J., Lapanje, A., Giongo, A., Kennedy, S., Aung, Y.-Y., Cattaneo, A., Davis-Richardson, A. G., Brown, C. T., Kort, R., Brumsack, H.-J., Schnetger, B., Chappell, A., Kroijenga, J., Beck, A., Schwibbert, K., Mohamed, A. H., Kirchner, T., de Quadros, P. D., Triplett, E. W., Broughton, W. J., and Gorbushina, A. A.: Microbial hitchhikers on intercontinental dust: catching a lift in Chad, The ISME Journal, 7, https://doi.org/10.1038/ismej.2012.152, 2013.

Feltracco, M., Barbaro, E., Kirchgeorg, T., Spolaor, A., Turetta, C., Zangrando, R., Barbante, C., and Gambaro, A.: Free and combined L-and D-amino acids in Arctic aerosol, Chemosphere, 220, 412-421, https://doi.org/10.1016/j.chemosphere.2018.12.147, 2019.

Filippo, P. D., Pomata, D., Riccardi, C., Buiarelli, F., Gallo, V., and Quaranta, A.: Free and combined amino acids in size-segregated atmospheric aerosol samples, Atmospheric Environment, 98, 179-189, https://doi.org/10.1016/j.atmosenv.2014.08.069, 2014.

https://doi.org/10.5194/egusphere-2024-2065
Preprint. Discussion started: 23 August 2024
© Author(s) 2024. CC BY 4.0 License.

Gazeau, F., Van Wambeke, F., Marañón, E., Pérez-Lorenzo, M., Alliouane, S., Stolpe, C., Blasco, T., Leblond, N., Zäncker, B., Engel, A., Marie, B., Dinasquet, J., and Guieu, C.: Impact of dust addition on the metabolism of Mediterranean plankton communities and carbon export under present and future conditions of pH and temperature, Biogeosciences, 18, 5423-5446, https://bg.copernicus.org/articles/18/5423/2021/, 2021.

Haan, D. O. D., Corrigan, A. L., Smith, K. W., Stroik, D. R., Turley, J. J., Lee, F. E., Tolbert, M. A., Jimenez, J. L., Cordova, K. E., and Ferrell, G. R.: Secondary Organic Aerosol-Forming Reactions of Glyoxal with Amino Acids, Environmental Science & Technology, 43, 2818-2824, https://doi.org/10.1021/es803534f, 2009.

Ho, K. F., Ho, S. S. H., Huang, R. J., Liu, S. X., Cao, J. J., Zhang, T., Chuang, H. C., Chan, C. S., Hu, D., and Tian, L.: Characteristics of water-soluble organic nitrogen in fine particulate matter in the continental area of China, Atmospheric Environment, 106, 252-261, https://doi.org/10.1016/j.atmosenv.2015.02.010, 2015.

Ianiri, H. L. and McCarthy, M. D.: Compound specific δ15N analysis of amino acids reveals unique sources and differential cycling of high and low molecular weight marine dissolved organic nitrogen, Geochimica et Cosmochimica Acta, 344, 24-39, https://doi.org/10.1016/j.gca.2023.01.008, 2023.

Jaber, S., Joly, M., Brissy, M., Leremboure, M., Khaled, A., Ervens, B., and Delort, A. M.: Biotic and abiotic transformation of amino acids in cloud water: experimental studies and atmospheric implications, Biogeosciences, 18, 1067-1080, https://doi.org/10.5194/bg-18-1067-2021, 2021.

Jaenicke, R.: Abundance of Cellular Material and Proteins in the Atmosphere, Science, 308, 73-73, https://doi.org/10.1126/science.1106335, 2005.

Kang, H., Xie, Z., and Hu, Q.: Ambient protein concentration in PM_{10} in Hefei, central China, Atmospheric Environment, 54, 73-79, https://doi.org/10.1016/j.atmosenv.2012.03.003, 2012.

Li, X., Zhang, Y., Shi, L., Kawamura, K., Kunwar, B., Takami, A., Arakaki, T., and Lai, S.: Aerosol Proteinaceous Matter in Coastal Okinawa, Japan: Influence of Long-Range Transport and Photochemical Degradation, Environmental Science & Technology, 56, 5256-5265, https://doi.org/10.1021/acs.est.1c08658, 2022a.

Li, Y., Zhang, H., Li, A., Zhang, J., and Du, S.: High time-resolved variations of proteins in PM2.5 during haze pollution periods in Xi'an, China, Environmental Pollution, 305, 119212, https://doi.org/10.1016/j.envpol.2022.119212, 2022b.

Liu, Q., Liu, Y., Zhao, Q., Zhang, T., and Schauer, J. J.: Increases in the formation of water soluble organic nitrogen during Asian dust storm episodes, Atmospheric Research, 253, 105486, https://doi.org/10.1016/j.atmosres.2021.105486, 2021.

Luo, L., Kao, S. J., Bao, H., Xiao, H., Xiao, H., Yao, X., Gao, H., Li, J., and Lu, Y.: Sources of reactive nitrogen in marine aerosol over the Northwest Pacific Ocean in spring, Atmospheric Chemistry and Physics, 18, 6207-6222, https://doi.org/10.5194/acp-18-6207-2018, 2018.

Mace, K. A., Kubilay, N., and Duce, R. A.: Organic nitrogen in rain and aerosol in the eastern Mediterranean atmosphere: An association with atmospheric dust, 108, https://doi.org/10.1029/2002JD002997, 2003.

Matos, J. T. V., Duarte, R. M. B. O., and Duarte, A. C.: Challenges in the identification and characterization of free amino acids and proteinaceous compounds in atmospheric aerosols: A critical review, TRAC Trends in Analytical Chemistry, 75, 97-107, https://doi.org/10.1016/j.trac.2015.08.004, 2016.

https://doi.org/10.5194/egusphere-2024-2065
Preprint. Discussion started: 23 August 2024
© Author(s) 2024. CC BY 4.0 License.

Matsumoto, K., Kim, S., and Hirai, A.: Origins of free and combined amino acids in the aerosols at an inland urban site in Japan, Atmospheric Environment, 259, 118543, https://doi.org/10.1016/j.atmosenv.2021.118543, 2021.

Matsumoto, K., Yamamoto, Y., Kobayashi, H., Kaneyasu, N., and Nakano, T.: Water-soluble organic nitrogen in the ambient aerosols and its contribution to the dry deposition of fixed nitrogen species in Japan, Atmospheric Environment, 95, 334-343, https://doi.org/10.1016/j.atmosenv.2014.06.037, 2014.

Matsumoto, K., Yamamoto, Y., Nishizawa, K., Kaneyasu, N., Irino, T., and Yoshikawa-Inoue, H.: Origin of the water-soluble organic nitrogen in the maritime aerosol, Atmospheric Environment, 167, 97-103, https://doi.org/10.1016/j.atmosenv.2017.07.050, 2017.

Mccarthy, M. D., Lehman, J., and Kudela, R.: Compound-specific amino acid δ 15 N patterns in marine algae: Tracer potential for cyanobacterial vs. eukaryotic organic nitrogen sources in the ocean, Geochimica et Cosmochimica Acta, 103, 104-120, https://doi.org/10.1016/j.gca.2012.10.037, 2013.

Mochizuki, T., Kawamura, K., and Aoki, K.: Water-Soluble Organic Nitrogen in High Mountain Snow Samples from Central Japan, Aerosol and Air Quality Research, 16, 632-639, https://doi.org/10.4209/aaqr.2015.04.0256, 2016.

Nakamura, T., Ogawa, H., Maripi, D. K., and Uematsu, M.: Contribution of water soluble organic nitrogen to total nitrogen in marine aerosols over the East China Sea and western North Pacific, Atmospheric Environment, 40, 7259-7264, https://doi.org/10.1016/j.atmosenv.2006.06.026, 2006.

Neff, J. C., Holland, E. A., Dentener, F. J., McDowell, W. H., and Russell, K. M.: The origin, composition and rates of organic nitrogen deposition: A missing piece of the nitrogen cycle?, Biogeochemistry, 57, 99-136, https://doi.org/10.1023/A:1015791622742, 2002.

Petroselli, C., Montalbani, E., La Porta, G., Crocchianti, S., Moroni, B., Casagrande, C., Ceci, E., Selvaggi, R., Sebastiani, B., Gandolfi, I., Franzetti, A., Federici, E., and Cappelletti, D.: Characterization of long-range transported bioaerosols in the Central Mediterranean, Science of the Total Environment, 763, 143010, https://doi.org/10.1016/j.scitotenv.2020.143010, 2021.

Samy, S., Robinson, J., Rumsey, I. C., Walker, J. T., Hays, M. D., Robinson, J., Rumsey, I. C., and Hays, M. D.: Speciation and trends of organic nitrogen in southeastern U.S. fine particulate matter (PM2.5), Journal of Geophysical Research: Atmospheres, 118, 1996-2006, https://doi.org/10.1029/2012JD017868, 2013.

Shi, J., Gao, H., Qi, J., Zhang, J., and Yao, X.: Sources, compositions, and distributions of water-soluble organic nitrogen in aerosols over the China Sea, Journal of Geophysical Research: Atmospheres, 115, https://doi.org/10.1029/2009JD013238, 2010.

Song, T., Wang, S., Zhang, Y., Song, J., Liu, F., Fu, P., Shiraiwa, M., Xie, Z., Yue, D., Zhong, L., Zheng, J., and Lai, S.: Proteins and Amino Acids in Fine Particulate Matter in Rural Guangzhou, Southern China: Seasonal Cycles, Sources, and Atmospheric Processes, Environmental Science & Technology, 51, 6773-6781, https://doi.org/10.1021/acs.est.7b00987, 2017.

Song, W., Liu, X.-Y., Hu, C.-C., Chen, G.-Y., Liu, X.-J., Walters, W. W., Michalski, G., and Liu, C.-Q.: Important contributions of non-fossil fuel nitrogen oxides emissions, Nature Communications, 12, 243, https://doi.org/10.1038/s41467-020-20356-0, 2021.

Song, W., Wang, Y.-L., Yang, W., Sun, X.-C., Tong, Y.-D., Wang, X.-M., Liu, C.-Q., Bai, Z.-P., and Liu, X.-Y.: Isotopic evaluation on relative contributions of major NOx sources to nitrate of $PM_{2.5}$ in Beijing, Environmental Pollution, 248, 183-190, https://doi.org/10.1016/j.envpol.2019.01.081, 2019.

https://doi.org/10.5194/egusphere-2024-2065
Preprint. Discussion started: 23 August 2024
© Author(s) 2024. CC BY 4.0 License.

Tan, S.-C., Shi, G.-Y., Shi, J.-H., Gao, H.-W., and Yao, X.: Correlation of Asian dust with chlorophyll and primary productivity in the coastal seas of China during the period from 1998 to 2008, Journal of Geophysical Research: Biogeosciences, 116, https://doi.org/10.1029/2010JG001456, 2011.

Tegen, I. and Schepanski, K.: The global distribution of mineral dust, IOP Conference Series: Earth and Environmental Science, 7, 012001, https://doi.org/10.1088/1755-1307/7/1/012001, 2009.

Triesch, N., van Pinxteren, M., Engel, A., and Herrmann, H.: Concerted measurements of free amino acids at the Cabo Verde islands: high enrichments in submicron sea spray aerosol particles and cloud droplets, Atmospheric Chemistry and Physics, 21, 163-181, https://doi.org/10.5194/acp-21-163-2021, 2021.

Tsagkaraki, M., Theodosi, C., Grivas, G., Vargiakaki, E., Sciare, J., Savvides, C., and Mihalopoulos, N.: Spatiotemporal variability and sources of aerosol water-soluble organic nitrogen (WSON), in the Eastern Mediterranean, Atmospheric Environment, 246, 118144, https://doi.org/10.1016/j.atmosenv.2020.118144, 2021.

Violaki, K. and Mihalopoulos, N.: Water-soluble organic nitrogen (WSON) in size-segregated atmospheric particles over the Eastern Mediterranean, Atmospheric Environment, 44, 4339-4345, https://doi.org/10.1016/j.atmosenv.2010.07.056, 2010.

Wedyan, M. A. and Preston, M. R.: The coupling of surface seawater organic nitrogen and the marine aerosol as inferred from enantiomer-specific amino acid analysis, Atmospheric Environment, 42, 8698-8705, https://doi.org/10.1016/j.atmosenv.2008.04.038, 2008.

Wu, C., Wang, G., Cao, C., Li, J., Li, J., Wu, F., Huang, R., Cao, J., Han, Y., Ge, S., Xie, Y., Xue, G., and Wang, X.: Chemical characteristics of airborne particles in Xi'an, inland China during dust storm episodes: Implications for heterogeneous formation of ammonium nitrate and enhancement of N-deposition, Environmental Pollution, 244, 877-884, https://doi.org/10.1016/j.envpol.2018.10.019, 2019.

Xu, Y., Xiao, H., Wu, D., and Long, C.: Abiotic and Biological Degradation of Atmospheric Proteinaceous Matter Can Contribute Significantly to Dissolved Amino Acids in Wet Deposition, Environmental Science & Technology, 54, 6551-6561, https://doi.org/10.1021/acs.est.0c00421, 2020.

Yamaguchi, Y. T. and McCarthy, M. D.: Sources and transformation of dissolved and particulate organic nitrogen in the North Pacific Subtropical Gyre indicated by compound-specific δ15N analysis of amino acids, Geochimica et Cosmochimica Acta, 220, 329-347, https://doi.org/10.1016/j.gca.2017.07.036, 2018.

Yang, Y., Bendle, J. A., Pancost, R. D., Yan, Y., Ruan, X., Warren, B., Lü, X., Li, X., Yao, Y., Huang, X., Yang, H., and Xie, S.: Leaf Wax and Sr-Nd Isotope Evidence for High-Latitude Dust Input to the Central South China Sea and Its Implication for Fertilization, Geophysical Research Letters, 48, e2020GL091853, https://doi.org/10.1029/2020GL091853, 2021.

Zamora, L. M., Prospero, J. M., and Hansell, D. A.: Organic nitrogen in aerosols and precipitation at Barbados and Miami: Implications regarding sources, transport and deposition to the western subtropical North Atlantic, 116, https://doi.org/10.1029/2011JD015660, 2011.

Zhang, J., Zhang, G. S., Bi, Y. F., and Liu, S. M.: Nitrogen species in rainwater and aerosols of the Yellow and East China seas: Effects of the East Asian monsoon and anthropogenic emissions and relevance for the NW Pacific Ocean, Global Biogeochemical Cycles, 25, https://doi.org/10.1029/2010GB003896, 2011.

Zhang, Q. and Anastasio, C.: Free and combined amino compounds in atmospheric fine particles (PM2.5) and fog waters from Northern California, Atmospheric Environment, 37, 2247-2258, https://doi.org/10.1016/S1352-2310(03)00127-4, 2003.

https://doi.org/10.5194/egusphere-2024-2065
Preprint. Discussion started: 23 August 2024
© Author(s) 2024. CC BY 4.0 License.

Zhang, Q., Anastasio, C., and Jimenez-Cruz, M.: Water-soluble organic nitrogen in atmospheric fine particles (PM2.5) from northern California, Journal of Geophysical Research, 107, AAC 3-1-AAC 3-9, https://doi.org/10.1029/2001JD000870, 2002.

Zhang, Z., Guan, H., Xiao, H., Liang, Y., Zheng, N., Luo, L., Liu, C., Fang, X., and Xiao, H.: Oxidation and sources of atmospheric NOx during winter in Beijing based on δ18O-δ15N space of particulate nitrate, Environmental Pollution, 276, 116708, https://doi.org/10.1016/j.envpol.2021.116708, 2021.

Zhu, R.-g., Xiao, H.-Y., Zhang, Z., and Lai, Y.: Compound-specific δ15N composition of free amino acids in moss as indicators of atmospheric nitrogen sources, Scientific Reports, 8, 14347, https://doi.org/10.1038/s41598-018-32531-x, 2018.

Zhu, R.-g., Xiao, H.-Y., Lv, Z., Xiao, H., Zhang, Z., and Xiao, H.: Nitrogen isotopic composition of free Gly in aerosols at a forest site, Atmospheric Environment, 222, 117179, https://doi.org/10.1016/j.atmosenv.2019.117179, 2020a.

Zhu, R.-g., Xiao, H.-Y., Zhu, Y., Wen, Z., Fang, X., and Pan, Y.: Sources and Transformation Processes of Proteinaceous Matter and Free Amino Acids in PM2.5, Journal of Geophysical Research: Atmospheres, 125, e2020JD032375, https://doi.org/10.1029/2020jd032375, 2020b.

Zhu, R. G., Xiao, H. Y., Luo, L., Xiao, H., Wen, Z., Zhu, Y., Fang, X., Pan, Y., and Chen, Z.: Measurement report: Hydrolyzed amino acids in fine and coarse atmospheric aerosol in Nanchang, China: concentrations, compositions, sources and possible bacterial degradation state, Atmospheric Chemistry and Physics, 21, 2585-2600, https://doi.org/10.5194/acp-21-2585-2021, 2021.